

RSC Advances



This is an *Accepted Manuscript*, which has been through the Royal Society of Chemistry peer review process and has been accepted for publication.

Accepted Manuscripts are published online shortly after acceptance, before technical editing, formatting and proof reading. Using this free service, authors can make their results available to the community, in citable form, before we publish the edited article. This *Accepted Manuscript* will be replaced by the edited, formatted and paginated article as soon as this is available.

You can find more information about *Accepted Manuscripts* in the [Information for Authors](#).

Please note that technical editing may introduce minor changes to the text and/or graphics, which may alter content. The journal's standard [Terms & Conditions](#) and the [Ethical guidelines](#) still apply. In no event shall the Royal Society of Chemistry be held responsible for any errors or omissions in this *Accepted Manuscript* or any consequences arising from the use of any information it contains.

Cite this: DOI: 10.1039/c0xx00000x

www.rsc.org/xxxxxx

ARTICLE TYPE

Synergistic effect between Pd and Re on Pd-Re/SBA-15 catalysts and their catalytic behavior in glycerol hydrogenolysis

Yuming Li,^a Huimin Liu,^a Lan Ma^{a,b} and Dehua He^{*a}

Received (in XXX, XXX) Xth XXXXXXXXX 20XX, Accepted Xth XXXXXXXXX 20XX

DOI: 10.1039/b000000x

Pd-Re/SBA-15 catalysts were prepared by impregnation method. The influence of interaction between Pd and Re in Pd-Re catalysts on glycerol hydrogenolysis was investigated. Pd and Re had interaction which was confirmed by H₂-TPR, XPS and EXAFS. In Pd-Re catalysts, Re showed higher oxidation state compared with mono-component Re catalyst. The mechanical mixed Pd+Re catalysts showed lower glycerol conversion than bi-component Pd-Re catalysts which suggested that the interaction of Pd and Re was very important in glycerol hydrogenolysis.

Introduction

In recent years, as the consumption of fossil fuels like coal, oil and natural gas growing rapidly, renewable and environmental friendly resources are eagerly to be developed [1]. Biodiesel which could offer great potential is one of these kinds of resources. It was produced by transesterification of vegetable oil or fatty acid esters with methanol or ethanol. The demand of biodiesel would increase to 100-300 EJ/y by 2050 [2]. At meantime, during the production of biodiesel, glycerol is formed as a by-product. But the traditional usage cannot satisfy the high accumulation, new ways should be found for this platform molecule material [3]. Hydrogenolysis of glycerol can produce 1,2-propanediol (1,2-PD) and 1,3-propanediol (1,3-PD) which are all high-value added chemicals. At present, 1,2-PD is produced mainly by hydrolysis of epoxypropane in petrochemical industry. It can be used in synthesis polyethers, unsaturated polyester resins and antifreeze products, as well as in food industry. On the other hand, 1,3-PD has highest value among the products of glycerol hydrogenolysis. Nowadays, it's usually produced by petrochemical routes from ethylene oxide or acrolein. 1,3-PD is mainly used to produce a kind of fiber PTT (polytrimethylene-terephthalate) which is widely used in industry. Meanwhile, it's also important in pharmaceuticals industry as a kind of drug intermediates. [4-5]

Many researches have been published for glycerol hydrogenolysis. Z. Xiao et al [6] used CuCr₂O₄ as catalyst in this reaction. 45.2% of glycerol conversion and 99.6% of selectivity to 1,2-PD were obtained under 130 °C and 2 MPa H₂ pressure. But most of non-noble metal Cu or Ni catalysts had no 1,3-PD production [7-8]. For noble metals, Ru [9], Pt [10] and Pd [11] were always used. In these noble metal based catalysts, 1,3-PD could be obtained. And from our previous studies and other papers [12-16], the addition of Re could increase the activities of noble metals. For Ru-Re [15-16] catalysts, the addition of Re increased

the conversions of glycerol from 6-32% to 50-60%, and the yields to 1,2-PD also increased. In this study, Re was added into Pd/SBA-15. And the addition of Re could increase the activity of Pd. As the content of Re increased, the conversion of glycerol also increased. Re and Pd may have an interaction and increase the activity of C-O bond cleavage. The preparation and reaction conditions were varied and the influences on the properties of Pd-Re catalysts were studied.

Experiments

Materials

PdCl₂ was purchased from Shenyang Nonferrous Metal Institute. HReO₄ (75-80% aqueous solution) was purchased from Alfa Aesar. P123 (EO₂₀PO₇₀EO₂₀, Mw=5800) was purchased from Sigma-Aldrich. Other materials (analytical reagents) were all bought from Beijing Chemical Reagent Company.

Catalyst preparation

SBA-15 was prepared with the method as references [17-18]. P123 was dissolved in HCl aqueous solution and the TEOS (tetraethylorthosilicate) was added and hydrolyzed for 20 h. After filtration, washed with deionized water until neutral and dried, the sample was calcined at 500 °C for 6 h to remove the template.

Pd-Re catalysts were all prepared by impregnation method. SBA-15 was impregnated with PdCl₂ which was dissolved in HCl aqueous solution, and HReO₄ aqueous solution at room temperature for 10 h with continuously stirring. After removing water by evaporation and drying at 110 °C overnight, the samples were directly reduced by pure hydrogen at 250 °C for 2 h. The obtained catalysts are denoted as xPd-yRe/SBA-15, where x and y meant the content of Pd and Re (quality content wt%), respectively. With the ICP analysis, the actual contents of Pd and Re in the fresh catalysts are nearly to their theoretical ones. With 5Pd-5Re/SBA-15 catalyst as an example, the actual content of Pd was 5.0 wt%, and the actual content of Re was 5.1 wt%.

RSC Advances Accepted Manuscript

For mechanical mixed Pd+Re catalysts, 10Pd/SBA-15 and 10Re/SBA-15 were reduced respectively and then mixed together by mechanical mixing (denoted as 10Pd+10Re). Another mechanical mixed catalyst (denoted as 5Pd+5Re) was prepared by the method the same as 10Pd+10Re (using 5Pd/SBA-15 and 5Re/SBA-15).

Catalyst Characterization

The structure properties of the catalysts, including pore volume, size distribution and specific surface area were characterized by N₂ adsorption/desorption with BET and BJH methods on a Micromeritics ASAP 2010C analyser. All samples were degassed at 300 °C before the characterization.

The crystall structures of all samples were characterized by X-ray diffraction (XRD) on a Rigaku D/max-RB diffractometer (powered at 40 kV and 200 mA).

The acidity of the catalysts were characterized by NH₃-TPD with Quantachrome CHEM-300 chemisorption instrument equipped with a quadrupole mass-spectrometer detector (Ametek Dymaxion, DM300 M Gas Analyser). 0.1 g of the sample was firstly treated at 250 °C with pure He gas (99.999%) for 2 h, and then cooled down to 100 °C to adsorb NH₃ with 2%NH₃/He gas at 100 °C for 0.5 h. After flowing in pure He gas at 100 °C for another 0.5 h to move the physical adsorption of NH₃, the temperature was increased from 100 °C to 750 °C at the rate of 15 °C/min.

The reduction behaviors of the catalysts were also characterized with H₂-TPR method on Quantachrome CHEM-300 chemisorption instrument. In a typical H₂-TPR, 0.1 g of the sample was firstly treated at 250 °C in pure Ar gas (99.999%) for 2 h. After the sample was cooled down to 30 °C, the Ar gas was switched into by-pass and changed into 5%H₂/Ar. The TCD detector was stabilized in 5%H₂/Ar at 30 °C, and then the gas switched into the sample tube again. During this process, the reduction peak of palladium at 30 °C would combine with a peak which caused by the residual pure Ar gas in the sample tube. This was recorded as Step I. After the TCD was stabled at 30 °C, the Step II of H₂-TPR was recorded by increasing the temperature from 30 °C into 500 °C at the rate of 15 °C/min.

The dispersion of Pd in Pd-Re catalysts was characterized by CO chemisorption. In a typical measurement, 0.1 g of the sample was reduced with 5%H₂/Ar at 250 °C for 2 h, and then cooled down to 30 °C in 99.999% He gas. After stabilized at 30 °C for 30 min, CO was pulsed for several times for the chemisorption and dispersion of Pd was calculated.

The high resolution transmission electron microscopy (HR-TEM) of the catalysts was taken on JEM-2010 JEOL with an energy dispersive spectrometer (EDS).

The X-ray photoelectron spectroscopy (XPS) was recorded by PHI Quantera SXM of ULVAC-PHI Inc. The binding energy

of all samples was calibrated with C 1s peak (284.6 eV).

Re L₃-edge extended X-ray absorption fine structure (EXAFS) was characterized on Beijing Synchrotron Radiation Facility (BSRF) 1W1B station.

Hydrogenolysis of glycerol

Glycerol hydrogenolysis was carried out in a 100 mL of stainless steel autoclave with a magnetic stirrer. For a typical reaction, 0.15 g Pd catalyst and 40 % glycerol aqueous solution were added into the autoclave. After sealing up the autoclave, 8MPa H₂ was purged to check leakage. Then 3 MPa H₂ was used to purge air for 3 times to remove the air in the autoclave. The autoclave was heated to 200 °C, and 8MPa H₂ was charged. Then the stirrer was started, and the reaction was carried on for 18 h. After reaction, the autoclave was cooled down to 5 °C and then the gas was decompressed. The gas phase products were analyzed by TCD gas chromatograph (Beijing Weisifu-GC 6890) and liquid phase products were analyzed by FID gas chromatograph (Lunan-SP 6890).

The conversion of glycerol and the selectivity to products were calculated based on following equations. The carbon balances of all reactions were maintained at 95±5%.

$$\text{Conversion}(\%) = \frac{\text{Sum of C mol of all products}}{\text{Added glycerol before reaction (C mol)}} \times 100\%$$

$$\text{Selectivity}(\%) = \frac{\text{C mol of each product}}{\text{Sum of C mol of all products}} \times 100\%$$

Results and discussion

The structure properties of xPd-5Re/SBA-15 catalysts

The structure properties of xPd-5Re/SBA-15 catalysts after reduced at 250 °C were measured by N₂ adsorption-desorption method. Fig. 1 (a) shows the the N₂ adsorption-desorption isotherms of xPd-5Re/SBA-15. All catalysts had type IV isotherms, which meant the mesoporous structure of SBA-15 had been maintained. The pore size distributions of xPd-5Re/SBA-15 are shown in Fig. 1 (b). All the catalysts had similar pore size distribution with SBA-15. The specific surface areas, pore volumes and average pore sizes of the samples are shown in Table 1. After impregnation and reduction, the specific surface area of xPd-5Re/SBA-15 became lower than that of SBA-15. 1Pd-5Re/SBA-15 had the largest specific surface area (784 m²/g), while 10Pd-5Re/SBA-15 had the smallest (610 m²/g). All catalysts had similar pore volume and average pore size.

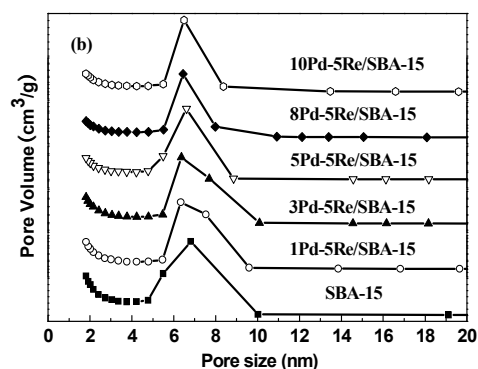
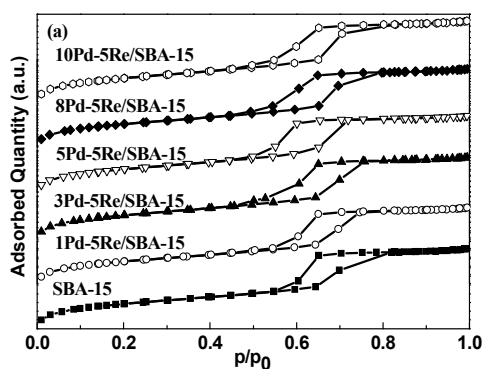
Table 1 Structure properties, dispersions and H₂ consumption of xPd-5Re/SBA-15

	S _{BET} (m ² /g)	V (cm ³ /g)	D _{BJH} (nm)	Dispersion of Pd (%) ^a	Step I H ₂ (mmol) ^b	Step II H ₂ (mmol) ^b	Total H ₂ (mmol) ^b
SBA-15	856	0.71	5.7	-	-	-	-
1Pd-5Re/SBA-15	784	0.66	5.6	31.7	-0.001	0.076	0.075
3Pd-5Re/SBA-15	730	0.61	5.7	19.6	0.047	0.059	0.105
5Pd-5Re/SBA-15	618	0.53	5.4	13.7	0.063	0.055	0.118
8Pd-5Re/SBA-15	638	0.55	5.6	11.1	0.109	0.039	0.149
10Pd-5Re/SBA-15	610	0.53	5.6	9.8	0.139	0.043	0.181
5Pd/SBA-15*	670	0.53	5.4	17.3	0.025	0.013	0.037
5Re/SBA-15*	705	0.59	5.4	-	-0.001	0.097	0.096

a: calculated from CO chemsorption

b: calculated from H₂-TPR

*: results from our previous paper [24]

Fig. 1 (a) N₂ adsorption-desorption isotherms and (b) pore size distribution of xPd-5Re/SBA-15

The structures and dispersions of xPd-5Re/SBA-15 catalysts

From the small angle XRD patterns of xPd-5Re/SBA-15 in Fig. 2 (a), it can be seen that all catalysts maintained the mesoporous structure of SBA-15. From the wide angle XRD patterns (Fig. 2 (b)), when the content of Pd was low (1%), the diffraction peaks of Pd⁰ were not clearly. As the content of Pd increased, the diffraction peaks of Pd(111) at 2θ = 40°, Pd(200) at 2θ = 46° and Pd(220) at 2θ = 68° were observed [19-21]. As the content of Pd increased from 1% to 10%, the dispersion of Pd decreased from 31.7% to 9.8%, which might be caused by the agglomeration of Pd at higher loading (Table 1).

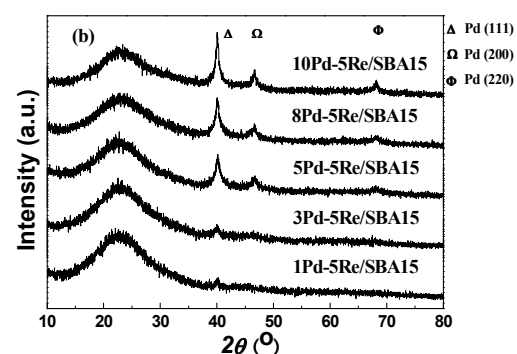
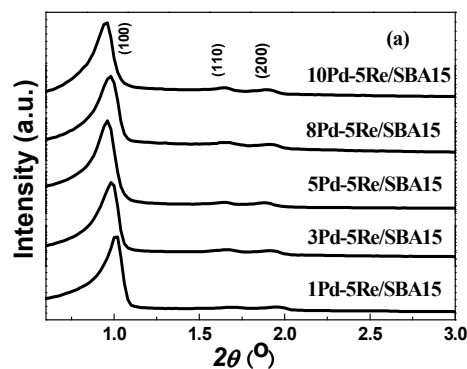


Fig. 2 (a) Small XRD patterns and (b) wide XRD patterns of xPd-5Re/SBA-15

The reduction behaviors of xPd-5Re/SBA-15 catalysts

The H₂-TPR profiles of xPd-5Re/SBA-15 are shown in Fig. 3, and the H₂ consumption results are listed in Table 1. It can be seen that the Step I of H₂-TPR of 1Pd-5Re/SBA-15 was same as that of SBA-15 blank indicating that there was nearly no Pd was reduced at 30 °C and all Pd might be interacted with Re for this sample. Other xPd-5Re/SBA-15 samples all showed higher consumption of H₂ than that of SBA-15 blank at 30 °C. For Step II of H₂-TPR, 1Pd-5Re/SBA-15 showed two broad reduction peaks at 150 °C and 200 °C, and it had no obviously decomposition peak of PdH at 100 °C [22-23]. As the content of Pd in xPd-5Re/SBA-15 increased to 3~10%, the peak at 150 °C shifted to lower temperature and the intensity of the peak became higher. For 3Pd-5Re/SBA-15 and 5Pd-5Re/SBA-15, the reduction peaks appeared at 130 °C and 220 °C, while for 8Pd-

5Re/SBA-15 and 10Pd-5Re/SBA-15, the reduction peaks became a broad peak in a wide temperature of 100~200 °C. The change of reduction behaviors of the catalysts might result in the change of the activity of Pd-Re catalysts. From the TPR results, it can be seen that all the catalysts (except 1Pd-5Re/SBA-15) had the reducible species that could be reduced at 30 °C and 130 °C (or 150 °C). As the content of Pd increased, the reduction temperature of the Pd-Re species decreased. Combining with the results of our group reported previously [24], the reduction species at 30 °C and 130 °C might be favourable the C-O bond cleavage and promoting the reaction. From H₂-TPR, the sum of H₂ consumption of 5Re/SBA-15 and 5Pd/SBA-15 (0.133 mmol) was higher than that of 5Pd-5Re/SBA-15 (0.118 mmol). It could be inferred that the oxidation state of Re in 5Pd-5Re/SBA-15 was different from that of Re in 5Re/SBA-15. XPS and EXAFS were introduced to characterize the oxidation state of Re in Pd-Re/SBA-15.

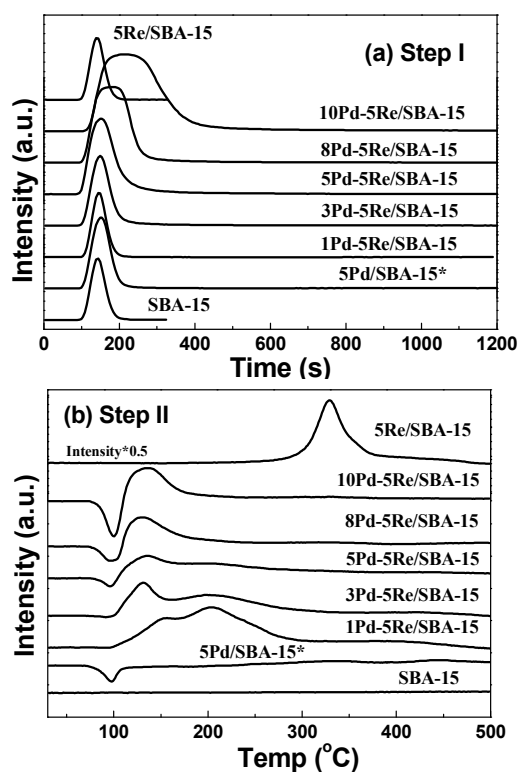


Fig. 3 (a) H₂-TPR profiles (Step I) and (b) H₂-TPR profiles (Step II) of xPd-5Re/SBA-15 (*: from our previous paper [24])

The oxidation states of Re in xPd-5Re/SBA-15 catalysts

With XPS analysis, the oxidation state of Re was characterized. All the results were calibrated by C 1s signal at 284.6 eV. Fig. 4 shows the XPS results of 5Re/SBA-15 after 500 °C calcination and after 250 °C reduction, respectively. For 5Re/SBA-15 after calcination in air, the binding energies (BE values) of Re were mainly at 48.9 eV and 46.8 eV, which means that the oxidation states of Re were in the range of 6⁺~7⁺ [25-26]. After reduction at 250 °C, the XPS spectrum changed a lot, and four peaks appeared in this sample. The BE values of Re were at 48.9 eV, 46.3 eV, 43.3 eV and 40.5 eV, indicating Re in 5Re/SBA-15 after

reduction had mixed oxidation states in the range of 0~7⁺. The peak at 40.5 eV (Re⁰) of the sample was very clearly, indicating that part of ReOx was reduced to Re⁰. But for the reduced 5Pd-5Re/SBA-15, as reported in our previous study [24], the XPS spectrum (Re 4f: 46.0 eV and 43.1 eV) of Re in the bi-component catalyst was very different from that of reduced mono-component 5Re/SBA-15 catalyst. The Re 4f peaks of the reduced 5Pd-5Re/SBA-15 were mainly at 46.0 eV and 43.1 eV, while the peak intensity of Re⁰ at 40.4 eV was very low [24]. This means the oxidation states of Re in 5Pd-5Re/SBA-15 after reduction were mainly in the range of 4⁺~7⁺. From XPS results of the samples, after reduction, the oxidation states of Re in bi-component catalyst were higher than that of Re in mono-component Re/SBA-15 catalyst. This result agreed with H₂-TPR results as discussed above.

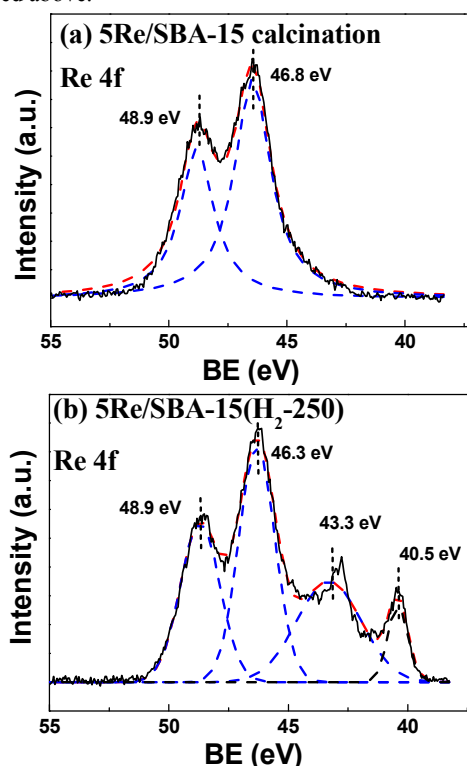


Fig. 4 XPS spectra of 5Re/SBA-15 (a) after calcination at 500 °C and (b) after reduction at 250 °C

In order to confirm the oxidation states of Re, XANES technique was also used for measuring Pd-Re catalysts. Re L₃-Edge was also analyzed by X-ray Absorption Fine Spectrum. Commercial samples of Re⁰ and ReO₃ were also used as comparison. From XANES spectra, the edge shift values of all samples were calculated and the results are shown in Table 2. From these results, it could be conferred that the valences of Re in 5Re/SBA-15 after reduction were between 0~6⁺, while the valence of Re in 5Pd-5Re/SBA-15 after reduction was a little higher than 6⁺. From k³-Weighted EXAFS oscillations of Re L₃-Edge EXAFS results (Fig. 5 (a)), the different intensity and frequency meant that the Re in 5Re/SBA-15 had different coordination environment compared with Re in 5Pd-5Re/SBA-15. The Fourier transform of k³-Weighted Re L₃-Edge EXAFS

(Fig. 5 (b)) results showed that there were two coordination peaks between 0.1~0.3 nm for Re in 5Re/SBA-15, while there was only one peak at 0.15 nm for Re in 5Pd-5Re/SBA-15. These differences meant the different coordination environments and local structures of Re in mono-component Re and bi-component Pd-Re catalysts.

Table 2 The edge shift values of Re L_{3} -Edge

	edge shift (eV)
Re	-1.93
ReO ₃	-4.66
5Re/SBA-15(H ₂ -250)	-3.32
5Pd-5Re/SBA-15(H ₂ -250)	-4.69

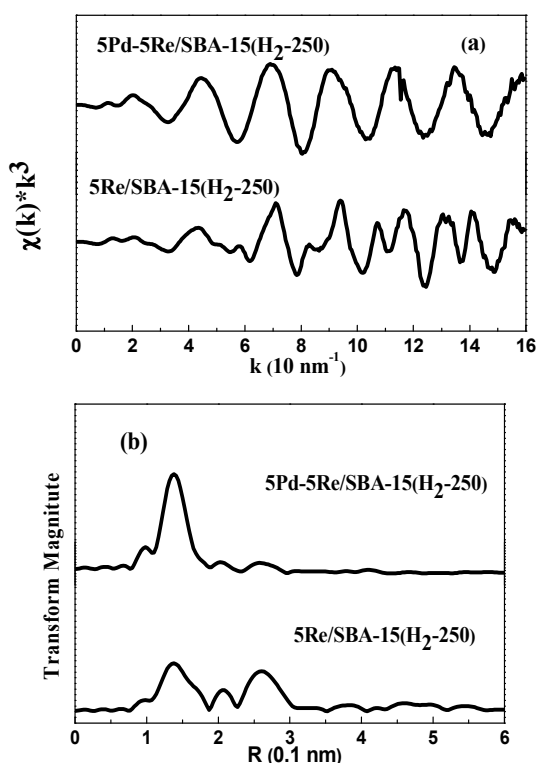


Fig. 5 (a) k^3 -Weighted EXAFS oscillations of Re L_{3} -Edge EXAFS and (b) the Fourier transform of k^3 -Weighted Re L_{3} -Edge EXAFS of Pd-Re catalysts

The catalytic performance of xPd-5Re/SBA-15 catalysts in glycerol hydrogenolysis

The catalytic performance of Pd-Re catalysts with different amounts of Pd is shown in Table 3. For mono-component Pd or Re catalyst, the conversion of glycerol was very low (1~3 %). For the bi-component Pd-Re catalysts, as the content of Pd increased from 1% to 8%, the conversion of glycerol increased from 15.0% to 72.2%. As the content of Pd further increased to 10%, the conversion of glycerol decreased somewhat (70.8%). With the increase of Pd amount, the selectivity to 1,2-PD and 1,3-PD decreased from 50~60% and 12.1% to 37.0% and 4.2%,

respectively, while the selectivity to 1-PO increased from 20~30% to 45.5%. From these results, it was suggested that there was an interaction between Pd and Re, which could influence not only the conversion of glycerol, but also the distribution of the products.

On the other hand, the spent 5Pd-5Re/SBA-15 catalyst was also recycled, and the recycle results of the catalyst in glycerol hydrogenolysis are listed in Table S1. It can be seen that from the results, the activity of the spent catalyst decreased a lot, and only 9.3%, compared with that of fresh one (40.7%). However, by calcining the spent catalyst at 500 °C and then reducing it at 250 °C in flowing H₂/N₂, the conversion of glycerol over regenerated 5Pd-5Re/SBA-15 was 28.8%, which was higher than that of unregenerated one (9.3%), and the product distribution was similar with the fresh one.

The spent 5Pd-5Re/SBA-15 catalyst was also characterized with XRD, TEM, TPH and TPO. From the small angle XRD patterns (Fig. S1 (a)), the spent 5Pd-5Re/SBA-15 still maintained the ordered mesoporous structure of SBA-15, but the intensity of SiO₂(111) peak decreased somewhat. From wide angle XRD pattern (Fig. S1 (b)), the peak of Pd(111) at $2\theta = 40^\circ$ became a little higher after reaction, which meant the particle size of Pd increased somewhat. From TEM images in Fig. S2, the average particle sizes of 5Pd-5Re/SBA-15 catalyst before and after reaction were 5.1 nm and 5.0 nm, respectively. While the particle size distribution of spent catalyst was 3~8 nm, this meant that some larger Pd-Re particles might be formed during the reaction.

From Table S1, the spent catalyst lost activity after glycerol hydrogenolysis reaction. However, after the calcination and reduction, the activity of the spent catalyst could be recovered to a certain extent. From this, it could be suspected that some organic species or carbon species might block the pores of the catalysts. TPH and TPO were used to characterize the carbon deposition in the spent catalyst, which are shown in Fig. S3 and S4.

From the results of TPH and TPO, it was suggested that the spent 5Pd-5Re/SBA-15 catalyst might be partly covered by some kinds of carbon deposition species after the reaction, which would cause the deactivation of the catalyst. But the calcination of the spent catalyst at 500 °C could remove the organic species deposition and recover the activity to the catalyst.

The effect of reduction temperatures on the catalytic performance and properties of 5Pd-5Re/SBA-15

From results mentioned above, Re in 5Pd-5Re/SBA-15 after reduction at 250 °C could still maintain at high oxidation state, and this might be due to the interaction of Pd and Re. Considering the reduction behaviors of 5Pd-5Re/SBA-15 in H₂-TPR, it could be suggested that the different reduction temperatures might lead to different activities. Therefore, the effect of different reduction temperatures on the activity of 5Pd-5Re/SBA-15 was checked, and results are shown in Table 4. From the results, it is clearly shown that when the 5Pd-5Re/SBA-15 was only dried at 110 °C without reduction, the conversion of glycerol was very low (only 7.2%). But the selectivity to 1,3-PD was the highest (21.3%). When 5Pd-5Re/SBA-15 was reduced

with H₂ at room temperature, the conversion of glycerol increased to 19.1% and the distribution of the products was similar to that of only dried 5Pd-5Re/SBA-15. As the reduction temperature increased into 150 °C, the conversion of glycerol got its maximum (50.7%) and the selectivity to 1,3-PD decreased to 8.3%. At the same time, the selectivities to 1,2-PD and 1-PO increased from about 30% to 45~55%. As the reduction temperature increased from 150 °C to 250 °C, the conversion of glycerol decreased to 40.7% and the selectivity to 1,2-PD increased to 59.9%. When the reduction temperatures were in the range of 250~550 °C, the glycerol conversions over 5Pd-5Re/SBA-15 and the dispersions of products were quite similar. If the reduction temperature continually increased to 650~750 °C, the conversions of glycerol sharply decreased from about 40% into about 21%.

From the H₂-TPR, it could be supposed that when the reduction temperature was below 130 °C, only the reducible Pd-

Re species at 30 °C was completely reduced, and other Pd-Re oxide that was only reduced at above 130 °C was maintained as oxides. This perhaps related to relatively lower activity of 5Pd-5Re/SBA-15. From XRD patterns in Fig. 6, 5Pd-5Re/SBA-15 without reduction showed no clearly diffraction peaks. When the catalyst was reduced at 25 °C, the diffraction peaks of Pd became clearly. When the reduction temperature increased to 150 °C, the reducible species in Pd-Re/SBA-15 below 130 °C could be totally reduced and the conversion of glycerol was the highest. Further increasing reduction temperature from 150 to 550 °C, the XRD diffraction peaks of Pd had nearly no changed (Fig. 6). After the reduction temperature increased to 750 °C, the conversion of glycerol decreased a lot, and from XRD pattern, the diffraction peaks of Pd disappeared and Pd-Si crystal component could be detected [27].

Table 3 Catalytic performance of xPd-5Re/SBA-15 in glycerol hydrogenolysis

	Conv. (%)	Select. (%)						
		CH ₄	C ₁₋₂ -OH	EG	1-PO	2-PO	1,2-PD	1,3-PD
5Pd/SBA-15	1.5	0.0	2.8	5.3	14.6	0.7	72.2	4.4
1Pd-5Re/SBA-15	15.0	1.1	0.8	0.9	25.0	1.8	58.3	12.1
3Pd-5Re/SBA-15	33.5	1.4	0.9	1.1	25.9	2.2	58.8	9.8
5Pd-5Re/SBA-15	40.7	2.0	1.4	1.8	24.6	2.1	59.9	8.2
8Pd-5Re/SBA-15	72.2	1.6	2.7	0.6	42.6	6.3	41.6	4.6
10Pd-5Re/SBA-15	70.8	1.8	2.8	0.9	45.5	7.8	37.0	4.2
5Re/SBA-15	3.1	0.0	1.7	1.7	38.7	1.5	49.6	6.7

Reaction Conditions: 0.15 g Pd catalyst, 40% Glycerol aqueous 10 mL, 200 °C, 8 MPa H₂, 18 h, 700 rpm.
C₁₋₂-OH: methanol and ethanol, EG: glycol, PO: propanol, PD: propanediols.

Table 4 The effect of reduction temperatures on catalytic performance of 5Pd-5Re/SBA-15 in glycerol hydrogenolysis

Treatment conditions (°C)	Conv. (%)	Select. (%)						
		CH ₄	C ₁₋₂ -OH	EG	1-PO	2-PO	1,2-PD	1,3-PD
Dry only (110)	7.2	0.3	1.1	1.1	46.3	0.8	29.2	21.3
H ₂ -25	19.1	0.8	0.6	0.6	50.9	1.4	29.6	16.0
H ₂ -50	23.5	0.9	0.8	0.6	41.6	1.4	41.7	12.9
H ₂ -110	40.2	0.9	1.1	0.9	38.4	2.7	46.5	9.5
H ₂ -150	50.7	1.4	1.2	0.9	39.0	3.6	45.6	8.3
H ₂ -250	40.7	2.0	1.4	1.8	24.6	2.1	59.9	8.2
H ₂ -350	42.2	1.4	1.3	1.2	24.8	2.8	61.0	7.5
H ₂ -450	41.7	0.9	1.6	1.5	22.0	3.5	62.9	7.7
H ₂ -500	41.4	1.8	1.5	1.4	25.3	3.5	57.0	9.5
H ₂ -550	39.9	2.1	2.1	2.1	22.1	3.9	60.9	6.9
H ₂ -650	30.6	1.7	1.7	2.7	18.8	2.5	65.0	7.6
H ₂ -750	21.3	2.2	1.0	3.8	15.3	1.4	66.9	9.4

Reaction Conditions: 0.15 g Pd catalyst, 40% Glycerol aqueous 10 mL, 200 °C, 8 MPa H₂, 18 h, 700 rpm.

Cite this: DOI: 10.1039/c0xx00000x

www.rsc.org/xxxxxx

ARTICLE TYPE

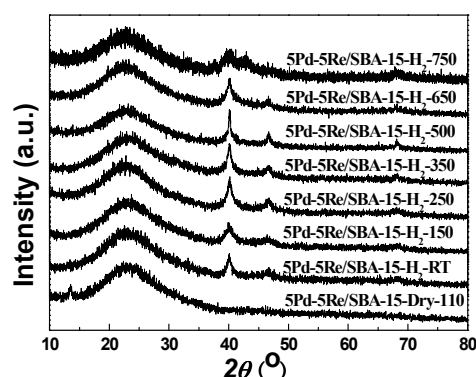


Fig. 6 XRD patterns of 5Pd-5Re/SBA-15 with different reduction temperatures

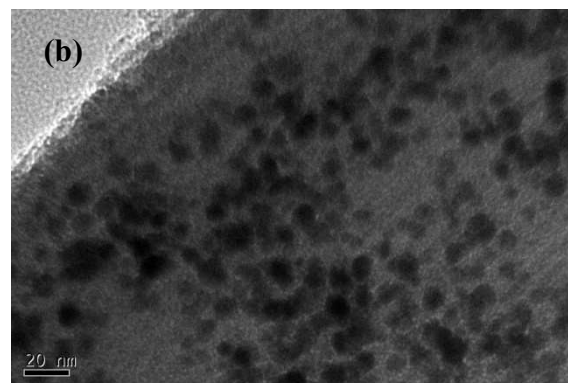
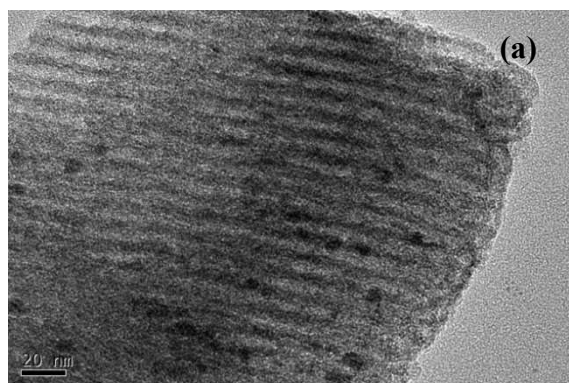


Fig. 7 TEM images of 5Pd-5Re/SBA-15 (a) reduced at 25 °C and (b) reduced at 750 °C

5

In order to confirm the morphology of 5Pd-5Re/SBA-15 prepared by different reduction temperatures, HR-TEM characterization was introduced. From TEM image of 5Pd-5Re/SBA-15 reduced at 25 °C (Fig. 7 (a)), the Pd-Re particles were all ball-like and the average particle size was 5 nm. With EDX analysis, both Pd and Re elements were confirmed in these particles. For 5Pd-5Re/SBA-15 reduced at 250 °C, the average particle size was also 5 nm, but the particles grew along the channel of SBA-15^[24] and showed rod-like shapes. When the reduction temperature increased to 750 °C, the TEM image (Fig. 7 (b)) showed a very different morphology from others. Pd-Re particles agglomerated into large and nonuniform particles with 5~16 nm scale, and the average particle size was 9.8 nm. Meanwhile, most of these particles stayed outside of SBA-15 channels.



25

From the characterization results of H₂-TPR, XRD and TEM of 5Pd-5Re/SBA-15 catalyst, when the reduction temperatures were below 110 °C, part of the Pd-Re oxide species could not be reduced and the activity of the catalyst was relatively low. The reducible species of Pd-Re could be fully reduced when the reduction temperatures were in the range of 150~550 °C. With the temperature variation in this range, the activities of 5Pd-5Re/SBA-15 were relatively high. However, when the reduction temperature became too high, the interaction between Pd and Re would be weakened and Pd-Si species was formed. This led the activity of 5Pd-5Re/SBA-15 became lower.

The effect of Pd and Re interaction on the catalytic performance of 5Pd-5Re/SBA-15 in glycerol hydrogenolysis

From the results mentioned above, Pd and Re in 5Pd-5Re/SBA-15 might have some interaction. To make sure the importance of Pd and Re interaction in glycerol hydrogenolysis, some mechanical mixing catalysts were prepared by mixing 10Pd/SBA-15 and 10Re/SBA-15 or 5Pd/SBA-15 and 5Re/SBA-15. The reaction results with these mechanical mixed catalysts are shown in Table 5. From these results, it can be seen that for 10Pd/SBA-15+10Re/SBA-15 and 5Pd/SBA-15+5Re/SBA-15 reduced at 250 °C, the conversions of glycerol were 12.8% and 20.7%, respectively. These conversions were much lower than that over 5Pd-5Re/SBA-15 prepared by co-impregnation method (40.7%). When the reduction temperature increased to 500 °C, the conversions of glycerol over two mechanical mixed catalysts decreased to 7.7% and 10.1%, respectively, and these were also much lower than that over co-impregnation 5Pd-5Re/SBA-15 reduced at 500 °C (41.4%). But the mechanical mixed catalysts still showed higher activities compared with mono-component Pd or Re catalyst (see Table 3). To study further, the sample of 10Pd/SBA-15+10Re/SBA-15 (denoted as 10Pd+10Re) was characterized by H₂-TPR and XRD.

From H₂-TPR profiles in Fig. 8, except PdH desorption peak at 100 °C, the reduction peaks of 10Pd+10Re were mainly at 30

°C and 350 °C, which were different from 5Pd-5Re/SBA-15. It was much like the overlap of TPR profiles of 5Pd/SBA-15 and 5Re/SBA-15 (Fig. 3). From this, it could be inferred that Pd and Re in mechanical mixed 10Pd+10Re catalyst had nearly no interaction.

Fig. 9 shows the XRD patterns of 10Pd+10Re catalyst and other catalysts. For 10Pd+10Re reduced at 250 °C, the intensity of diffraction peak of Pd⁰ was a little higher than that of Pd⁰ on 5Pd-5Re/SBA-15, and the diffraction peaks of Re⁰ could be clearly observed. After reduced at 500 °C, the intensity of diffraction peaks of Pd⁰ increased a lot, which meant that higher reduction temperatures would lead to bigger Pd particles. Meanwhile, the diffraction peaks of Re⁰ were also very clearly. These were different from 5Pd-5Re/SBA-15. As the reduction temperature of 5Pd-5Re/SBA-15 increased from 250 °C to 500 °C, the intensity of Pd⁰ diffraction peaks changed a little, and there was no obvious diffraction peak of Re⁰. It is suggested from XRD patterns that Pd and Re components in the mechanical mixed catalysts had no interaction, while ReOx on the mechanical mixed catalysts could be easily reduced.

Therefore, with the comparison of Pd-Re catalysts and mechanical mixed Pd+Re catalysts, it can be seen that the Pd and Re interaction was very important in glycerol hydrogenolysis. With this interaction, Pd-Re bi-component catalysts could have higher activities. To make sure this speculation, 1Pd-xRe/SBA-15 catalysts with different Re amounts were also prepared, and reduced in H₂ at 250 °C or 500 °C before using in the reaction.

From the TPR profiles in Fig. 10, it can be seen that the reduction properties of 1Pd-xRe/SBA-15 were different from that of mono-component Pd or Re catalyst. The two main reduction peaks of each catalysts appeared between 100~250 °C. This suggested that even when the content of Re increased to 15%, Pd and Re in 1Pd-xRe/SBA-15 still had interaction. The reaction

results (Table 6) showed that when the reduction temperature was 250 °C, the conversion of glycerol increased from 6.5% to 40.1% as the content of Re increased from 1% to 10%. For the distribution of the products, the selectivity to 1,2-PD decreased from 77.2% to 38.9%, while the selectivity to 1-PO and 1,3-PD increased from 7.6% and 7.2% to 45.5% and 10.1%, respectively. When the reduction temperature increased from 250 °C to 500 °C, the activities of 1Pd-xRe/SBA-15 catalysts changed a lot. For 1Pd-1Re/SBA-15 and 1Pd-5Re/SBA-15 catalysts, the increase of reduction temperature had little effect on the conversion of glycerol and the products distribution. But for 1Pd-10Re/SBA-15 and 1Pd-15Re/SBA-15 catalysts, the increase of reduction temperature made the conversion of glycerol decrease from 38.8% and 40.1% to 21.5% and 25.8%, respectively. For the products distribution, the selectivity to 1,2-PD maintained at about 50% which was higher than that of 250 °C reduced catalyst.

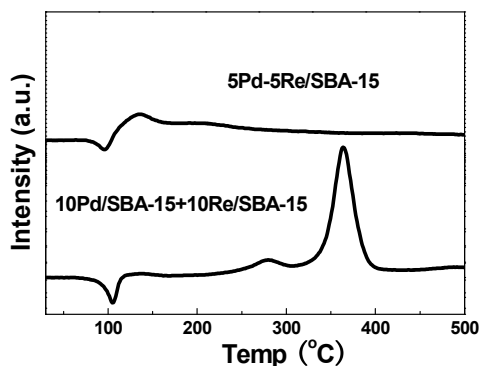


Fig. 8 Comparison of H₂-TPR profiles of Pd-Re/SBA-15 with Pd/SBA-15 + Re/SBA-15

Table 5 Comparison of the catalytic performance of Pd-Re/SBA-15 with mechanical mixed Pd/SBA-15 + Re/SBA-15 catalysts in glycerol hydrogenolysis

	Reduction Temp (°C)	Conv. (%)	Select. (%)						
			CH ₄	C ₁₋₂ -OH	EG	1-PO	2-PO	1,2-PD	1,3-PD
5Pd-5Re/SBA-15 ^a	250	40.7	2.0	1.4	1.8	24.6	2.1	59.9	8.2
5Pd/SBA-15+5Re/SBA-15 ^b	250	20.7	1.5	1.6	3.0	24.9	3.9	61.0	4.0
10Pd/SBA-15+10Re/SBA-15 ^c	250	12.8	1.5	1.6	1.4	22.6	4.0	59.4	9.5
5Pd-5Re/SBA-15 ^a	500	41.4	1.8	1.5	1.4	25.3	3.5	57.0	9.5
5Pd/SBA-15+5Re/SBA-15 ^b	500	10.1	1.3	1.5	4.4	24.8	3.9	59.6	4.6
10Pd/SBA-15+10Re/SBA-15 ^c	500	7.7	1.2	1.0	3.4	12.1	2.2	72.9	7.2

Reaction Conditions:

(a) 0.15 g Pd catalyst, 40% Glycerol aqueous 10 mL, 200 °C, 8 MPa H₂, 18 h, 700 rpm.

(b) 0.15 g Pd+0.15 g Re catalysts, 40% Glycerol aqueous 10 mL, 200 °C, 8 MPa H₂, 18 h, 700 rpm.

(c) 0.075 g Pd+0.075 g Re catalysts, 40% Glycerol aqueous 10 mL, 200 °C, 8 MPa H₂, 18 h, 700 rpm.

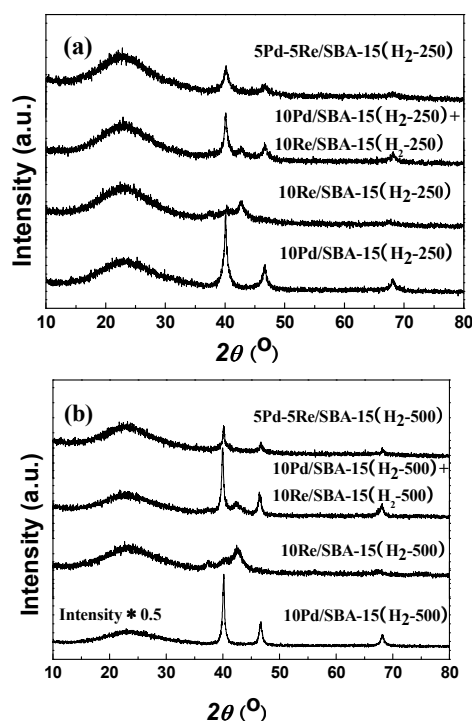


Fig. 9 Comparison of XRD patterns of Pd-Re/SBA-15 with Pd/SBA-15 + Re/SBA-15

(a) reduced at 250 °C, (b) reduced at 500 °C

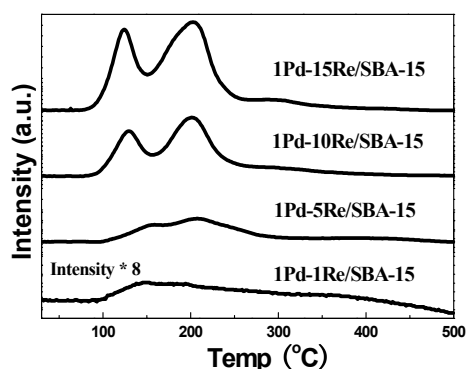


Fig. 10 H₂-TPR profiles of 1Pd-xRe/SBA-15

XRD patterns of 1Pd-xRe/SBA-15 reduced at 250 °C and 500 °C are shown in Fig. 11. It clearly shows that when the reduction temperature was 250 °C, there were no obvious diffraction peaks of Pd and Re, even when the content of Re was 15%. This indicated that for 1Pd-xRe/SBA-15 reduced at 250 °C, Pd and Re had some interaction. When the reduction temperature increased from 250 °C to 500 °C, for 1Pd-1Re/SBA-15 and 1Pd-5Re/SBA-15, there were still no Pd and Re diffraction peaks. This suggested that the interaction between Pd and Re was still maintained and the conversion of glycerol over these two catalysts had little changes compared with those of 250 °C reduced samples. But for 1Pd-10Re/SBA-15 and 1Pd-15Re/SBA-15, reduction temperature at 500 °C made ReOx being reduced into Re⁰ ($2\theta = 40.5^\circ$ and 42.9° , as shown in Fig. 11), which could be observed from the XRD patterns. The appearance of Re⁰ also meant that the Pd and Re interaction was partly weakened, which made the conversion of glycerol decreased. From above, Pd and Re interaction in bi-component catalysts played an important role in glycerol hydrogenolysis.

The effect of Pd and Re interaction on glycerol dehydration and acetol hydrogenation

From references [28-29], there are two main steps in glycerol hydrogenolysis, including glycerol dehydration to acetol and acetol hydrogenation to 1,2-PD. For researching the behaviors of Pd-Re catalysts in the dehydration and hydrogenation, 5Pd-5Re/SBA-15, 5Pd/SBA-15 and 5Re/SBA-15 catalysts were used in these two reactions. The results are listed in Table 7. For glycerol dehydration, the conversions of glycerol over mono-component Pd and Re catalysts were 7.0% and 5.6%, respectively. Meanwhile, the conversion of glycerol over 5Pd-5Re/SBA-15 was 26.5%, which was higher than that of mono-component Pd or Re catalyst. In glycerol dehydration, the main product was acetol. For 5Pd/SBA-15 and 5Re/SBA-15, the selectivity to acetol was 74.4% and 89.0%, respectively. For 5Pd-5Re/SBA-15, the selectivity to acetol was only 59.2%, which was lower than that of mono-component Pd or Re catalyst. While, the selectivity to 1,2-PD (25.3%) was higher than that of 5Pd/SBA-15 (16.4%) or 5Re/SBA-15 (5.8%).

Table 6 The catalytic performance of 1Pd-xRe/SBA-15 in glycerol hydrogenolysis

	Conv. (%)	Select. (%)						
		CH ₄	C ₁₋₂ -OH	EG	1-PO	2-PO	1,2-PD	1,3-PD
1Pd-1Re/SBA-15(H ₂ -250)	6.5	0.9	0.8	5.4	7.6	0.8	77.2	7.2
1Pd-5Re/SBA-15(H ₂ -250)	15.0	1.1	0.8	0.9	25.0	1.8	58.3	12.1
1Pd-10Re/SBA-15(H ₂ -250)	38.8	1.2	0.6	0.4	39.5	2.5	45.5	10.3
1Pd-15Re/SBA-15(H ₂ -250)	40.1	1.3	0.6	0.9	45.5	2.6	38.9	10.1
1Pd-1Re/SBA-15(H ₂ -500)	5.6	0.0	1.1	4.0	11.5	1.4	75.4	6.6
1Pd-5Re/SBA-15(H ₂ -500)	15.2	1.3	1.0	2.9	24.9	2.0	57.3	10.5
1Pd-10Re/SBA-15(H ₂ -500)	21.5	0.5	0.8	2.1	32.8	2.2	51.4	10.2
1Pd-15Re/SBA-15(H ₂ -500)	25.8	0.9	0.7	0.8	34.4	2.3	51.3	9.6

Reaction Conditions: 0.15 g Pd catalyst, 40% Glycerol aqueous 10 mL, 200 °C, 8 MPa H₂, 18 h, 700 rpm.

Cite this: DOI: 10.1039/c0xx00000x

www.rsc.org/xxxxxx

ARTICLE TYPE

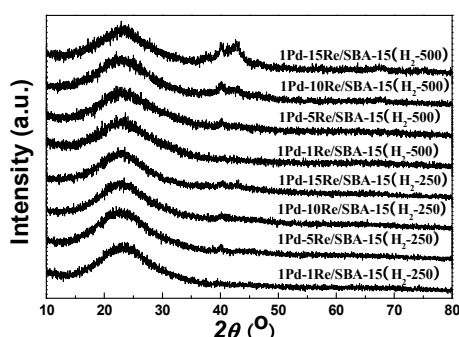


Fig. 11 XRD patterns of 1Pd-xRe/SBA-15 with different reduction temperatures

For acetol hydrogenation reaction, the bi-component 5Pd-5Re/SBA-15 also showed high conversion. For 5Pd/SBA-15, the conversion of acetol was the lowest (3.8%). And 21.3% of acetol conversion was got over 5Re/SBA-15, which was a little higher than that of 5Pd/SBA-15. For bi-component 5Pd-5Re/SBA-15, the conversion of acetol reached 86.0%. This was the highest among the three catalysts. For all catalysts, the selectivities to 1,2-PD were all higher than 90%.

From these results, bi-component Pd-Re catalysts showed higher performance in both glycerol dehydration and acetol hydrogenation reactions. These results were in accordance with the higher performance of Pd-Re catalysts in glycerol hydrogenolysis. Besides, the mechanical Pd+Re had a better activity than mono-component Pd catalyst. This might be caused by the acidity of ReOx, which could promote the dehydration step^[24]. From above, the synergism of Pd and Re interaction and acidity of ReOx lead Pd-Re bi-component catalysts more effective in glycerol hydrogenolysis.

Conclusions

Bi-component Pd-Re catalysts had higher activity than mono-component Pd or Re catalyst. With the addition of Re component, Pd particles were grown along the SBA-15 channels and the average particle size became smaller. Meanwhile, with the existence of Pd component, ReOx could maintain at higher oxidation state. Pd and Re interaction play an important role in glycerol hydrogenolysis and could promote both glycerol dehydration and acetol hydrogenation steps.

Table 7 The results of glycerol dehydration over Pd-Re catalysts

Reaction		Conv. (%)	Select. (%)					
			C ₁₋₂ -OH	1-PO	2-PO	1,2-PD	1,3-PD	Acetol
5Pd/SBA-15	Glycerol dehydration ^a	7.0	6.7	2.0	0.0	16.4	0.5	74.4
5Pd-5Re/SBA-15	Glycerol dehydration ^a	26.5	6.3	8.0	0.1	25.3	1.1	59.2
5Re/SBA-15	Glycerol dehydration ^a	5.6	2.5	1.7	0.2	5.8	0.7	89.0
SBA-15	Glycerol dehydration ^a	n.d.						
5Pd/SBA-15	Acetol hydrogenation ^b	3.8	2.4	1.9	1.3	94.4	0.0	-
5Pd-5Re/SBA-15	Acetol hydrogenation ^b	86.0	0.5	2.4	5.5	91.6	0.0	-
5Re/SBA-15	Acetol hydrogenation ^b	21.3	0.7	0.9	0.2	98.3	0.0	-
SBA-15	Acetol hydrogenation ^b	1.0	1.5	2.5	4.5	91.5	0.0	-

Reaction Conditions^a: 0.15 g Pd or 0.15 g Re catalyst, 40% Glycerol aqueous 10 mL, 200 °C, 8 MPa N₂, 18 h, 700 rpm.

Reaction Conditions^b: 0.15 g Pd or 0.15 g Re catalyst, 40% Glycerol aqueous 10 mL, 200 °C, 8 MPa H₂, 1 h, 700 rpm

Acknowledgement

This work is supported by the National Natural Science Foundation of China (No. 21033004, 20973098).

Notes and references

^a Innovative Catalysis Program, Key Lab of Organic Optoelectronics & Molecular Engineering of Ministry of Education, Department of Chemistry, Tsinghua University, Beijing 100084, China Fax: 86-10-62773346; Tel: 86-10-62773346; E-mail: hedeh@mail.tsinghua.edu.cn

^b Institute of Chemical Defence, Beijing 102205, China

† Electronic Supplementary Information (ESI) available: [details of any supplementary information available should be included here]. See DOI: 10.1039/b000000x/

[1] M. S. Singhvi, S. Chaudhari and D. V. Gokhale, *RSC Adv.*, 2014, **4**, 8271.

[2] Technology roadmap biofuels for transport. *International Energy Agency*. 2011.

[3] Y. Wang, J. Zhou and X. Guo, *RSC Adv.*, 2015, **5**, 74611.

[4] A. Behr, J. Eilting, K. Irawadi, J. Leschinski and F. Lindner, *Green Chem.*, 2008, **10**, 13.

[5] J. Wang, G. Yao, Y. Wang, H. Zhang, Z. Huo and F. Jin, *RSC Adv.*, 2015, **5**, 51435.

[6] Z. Xiao, J. Xiu, X. Wang, B. Zhang, C. T. Williams, D. Su and C. Liang, *Catal. Sci. Technol.*, 2013, **3**, 1108.

[7] A. Bienholz, F. Schwab and P. Claus, *Green Chem.*, 2010, **12**, 290.

[8] A. Y. Yin, X. Y. Guo, W. L. Dai and K. N. Fan, *Green Chem.*, 2009, **11**, 1514.

[9] N. Hamzah, N. M. Nordin, A. H. A. Nadzri, Y. A. Nik, M. B. Kassim and M. A. Yarmo, *Appl. Catal. A: Gen.*, 2012, **419-420**, 133.

[10] T. Kurosaka, H. Maruyama, I. Naribayashi and Y. Sasaki, *Catal. Commun.*, 2008, **9**, 1360.

[11] S. X. Xia, Z. L. Yuan, L. N. Wang, P. Chen and Z. Y. Hou, *Appl. Catal. A: Gen.*, 2011, **403**, 173.

- [12] O. Daniel, A. DeLaRiva, E. Kunkes, A. Datye, J. Dumesic and R. Davis, *ChemCatChem*, 2010, **2**, 1107.
- [13] Y. Shinmi, S. Koso, T. Kubota, Y. Nakagawa and K. Tomishige, *Appl. Catal. B: Environ.*, 2010, **94**, 318.
- 5 [14] Y. Nakagawa, X. Ning, Y. Amada and K. Tomishige, *J. Catal.*, 2010, **272**, 191.
- [15] L. Ma, D. H. He and Z. Li, *Catal. Commun.*, 2008, **9**, 2489.
- [16] L. Ma and D. H. He, *Catal. Today*, 2012, **149**, 148.
- [17] W. Zhou and D. H. He, *Chem. Commun.*, 2008, **9**, 5839.
- 10 [18] W. Zhou and D. H. He, *Green Chem.*, 2009, **11**, 1146.
- [19] Y. Feng, W. Xue, H. Yin, M. Meng, A. Wang and S. Liu, *RSC Adv.*, 2015, **5**, 106918.
- [20] J. Feng, X. Ma, Y. He, D. G. Evans and D. Li, *Appl. Catal. A: Gen.*, 2012, **413-414**, 10.
- 15 [21] X. Liang, C. Liu and P. Kuai, *Green. Chem.*, 2008, **10**, 1318.
- [22] N. Babu, N. Lingaiah, R. Gopinath, P. Reddy and P. Prasad, *J. Phys. Chem. C.*, 2009, **111**, 6447.
- [23] R. P´erez-Hern´andez, A. Avenda˜no, E. Rubio and V. Rodr´ıguez-Lugo, *Top. Catal.*, 2011, **54**, 572.
- 20 [24] Y. Li, H. Liu, L. Ma and D.H He, *RSC Adv.*, 2014, **4**, 5503.
- [25] J. Okal, W. Tylus and L. Kepinski, *J. Catal.*, 2004, **225**, 498.
- [26] F. John, F. William, E. Peter and D. Kenneth, *Handbook of X-ray Photoelectron Spectroscopy*. Minnesota, USA, 1995.
- 25 [27] W. Juszczyk, Z. Karpiński, D. Łomot and J. Pielaszek, *J. Catal.*, 2003, **220**, 229.
- [28] Z.M. Zhou, X. Li, T. Y. Zeng, W. B. Hong, Z. M. Cheng and W. K. Yuan, *Chin. J. Chem. Eng.*, 2010, **18**, 384.
- [29] Y. Kusunoki, T. Miyazawa, K. Kunimori and K. Tomishige, *Catal. Commun.*, 2005, **10**, 645.
- 30
- 35

Graphical abstract

